

Cased Hole Flexural Modes in Anisotropic Formations

Ping'en Li¹, Xianyue Su^{1,2} and Youquan Yin¹

Abstract: Based on the perturbation method, for flexural wave in cased hole in anisotropic formation, the alteration in the phase velocity caused by the differences in elastic constants between anisotropic formation of interest and a reference, or unperturbed isotropic formation is obtained. Assuming the cased hole is well bonded, the Thomson-Haskell transfer matrix method is applied to calculate the dispersion relation of flexural wave in cased hole in unperturbed isotropic formation. Both the cases of a fast and slow formation are considered where the symmetry axis of a transversely isotropic (TI) formation makes an angle with the cased hole axis, the dispersion of the phase velocity of the flexural mode in cased holes is studied. The corresponding dispersion curves of flexural wave in open hole are presented simultaneously for comparison. The computational results indicate that because of the influence of the casing, the flexural wave dispersion curves in cased hole in both fast and slow TI formations all almost tend toward an identical Stoneley wave velocity at higher frequency. The casing and the cement affect the form as well as the cut-off frequency of flexural wave dispersion curves more greatly in slow TI formation than in fast TI formation. At a frequency high enough, the flexural and the Stoneley waves reach the appropriate Scholte wave velocity in both the open hole and cased hole situation.

Keyword: Anisotropic formation, azimuthally anisotropic, cased hole, flexural mode, perturbation integral method, Thomson-Haskell method, dispersion curves

1 Introduction

The sonic logging is an important logging method and has been widely applied in many fields such as oil exploration, oil development and engineering geophysics. In order to design and develop an effective sonic logging instrument to acquire the accurate information of formation as well as the borehole from the sonic logging signal, the propagation of acoustic wave in borehole has been and still is extensively studied. In the past years, significant achievements have been obtained in the field of borehole acoustics. For isotropic elastic formation, the equations of motion can be decoupled and solved analytically by introducing displacement potential functions, thus it has been studied thoroughly for the borehole modes in isotropic formation. But usually, the formation is anisotropic, and the wave propagation problem in general anisotropic solid is complicated. The exact analytical solution cannot be obtained, which brings much difficulties to study the borehole waves in anisotropic formation. Therefore, the approximate method and pure numerical approach are very important. For general homogeneous anisotropic medium, an effective meshless method based on the local Petrov-Galerkin approach is proposed by Sladek [Sladek J, Sladek V, and Atluri (2004)] for solution elastodynamic problems. Subsequently, Atluri [Atluri, Liu, Han (2006)] developed a mixed finite difference method within the framework of the meshless local Petrov-Galerkin approach for solving solid mechanics problems. Later, a new numerical algorithm based on meshless local Petrov-Galerkin approach and modified moving least square method was proposed by Gao [Gao, Liu K, Liu Y (2006)] for analyzing the wave propagation and dynamic fracture problems in elastic media. For borehole problems, Ellef-

¹ LTCS, Department of Mechanics and Aerospace Engineering, Peking University, Beijing, 100871, P.R.China

² Corresponding author, Tel.: +86 010 6275 9378; Fax.: +86 010 6275 1812. E-mail address: xysu@mech.pku.edu.cn

sen [Ellefsen, Cheng, and Toksoz (1991)] investigated the dispersion curves of borehole modes in weak anisotropic formation using perturbation theory established on variational calculus and Hamilton's principle. Applying finite difference method, Leslie and Randall [Leslie and Randall (1992)], Liu and Sinha [Liu and Sinha (2003)] computed and analyzed the full wave acoustic fields in various complicated borehole model. Considering borehole waves decay away from the borehole, Sinha and Norris [Sinha, Norris, and Chang (1994), Norris and Sinha (1996)] proposed a perturbation integral procedure to study the Stoneley and flexural wave dispersion curves as well as excitation characters when the symmetry axis of the anisotropic formation makes an angle with the borehole axis. Zhang and Wang [Zhang and Wang (1996)] introduced three perturbation variables to denote the deviation in elastic constants between transversely isotropic (TI) formation of interest and a reference isotropic formation. Using perturbation method, the exact zero-order as well as the first-order approximate solutions of the wave field outside and inside the borehole is obtained when the symmetry axis of TI formation is perpendicular to the borehole axis. Subsequently, this method is further extended to study the borehole wave in anisotropic two-phase media [Zhang and Wang (2000)]. However, all of the above studies is focused on the open hole case. For the borehole modes in cased hole, the effects of the casing and cement properties on modes in isotropic formation have been extensively discussed by Tubman [Tubman, Cheng, and Toksoz (1984), Tubman, Cheng, Cole, and Toksoz (1986)] and Schmitt [Schmitt (1988), (1993)]. Recently, Li et al. [Li, Wang, Liu, Cao, Lu, Xie, Liu, and Lu (2006)] extended the perturbation integral method to the cased hole system and investigated the acoustoelastic effect on cased hole guide waves in stressed formation, where the formation is isotropic.

In this paper, the perturbation method proposed by Sinha and Norris [Sinha and Norris (1994)] is applied to the situation of well bonded cased hole for study of the dispersion of phase velocity of the flexural mode in anisotropic forma-

tion. Before computing the perturbation integral, the Thomsen-Haskell transfer matrix method is adopted to solve the dispersion relation of cased hole flexural waves in reference isotropic formation. Numerical examples are provided for both fast and slow TI formation where the symmetry axis of a TI formation makes an angle with the cased hole axis. The flexural wave dispersion curve of cased hole in fast and slow formations with different inclinations with respect to the TI symmetry axis are presented. The computational results show that the influence of the casing on flexural wave dispersion in cased hole is greater in slow TI formation than in fast TI formation. Compare to the corresponding flexural modes in open hole, the flexural waves in cased hole have the higher cut-off frequency, and the high-frequency asymptotes of dispersion curves all tend toward an identical casing-fluid interface Stoneley wave speed approximately. The flexural wave as well as Stoneley wave both in open hole and cased hole reach the appropriate Scholte wave velocity at the high enough frequency.

2 Formulation

A fluid-filled cased hole is a radially layered structure composed of the coaxial casing and the cement sheath annuli surrounding a fluid cylinder. A cylindrical coordinates is adopted as shown in Figure 1. The origin of coordinates is in the center of the cased hole. There are two interfaces: the first one between the casing and the cement sheath, and the second one between the cement sheath and the formation, which are called as the first and the second interface, respectively.

To the cased hole-formation system, the innermost fluid in the cased hole is the first layer, and the outermost infinite anisotropic elastic formation is the fourth layer. Both the casing and the cement sheath are isotropic. They are the second and the third layer, respectively. ρ_i ($i = 1, 2, 3, 4$) and R_i ($i = 1, 2, 3$) are the density and outer radius of each layer, respectively. The velocity of longitudinal wave and shear wave in each layer is v_{pi} ($i = 1, 2, 3$) and v_{si} ($i = 2, 3$), respectively, where the subscript "i" denotes the layer number. Assuming there is a m order multipole sonic source

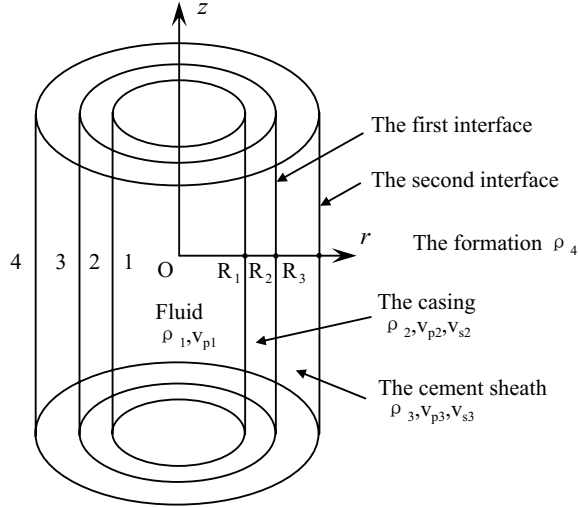


Figure 1: A fluid-filled cased hole model

in the center of the cased hole, the equations of motion are satisfied in each layer.

For isotropic elastic media, introducing the displacement potential functions, the displacements are

$$\mathbf{u}_1 = \nabla\varphi_1, \quad \mathbf{u}_i = \nabla\varphi_i + \nabla \times (\chi_i \hat{z}) + \nabla \times \nabla \times (\eta_i \hat{z}), \quad (i = 2, 3) \quad (1)$$

where \hat{z} is the axial unit vector, φ_i ($i = 1, 2, 3$) and χ_i, η_i ($i = 2, 3$) are displacement potential functions.

Ignoring the body force, the wave equation in fluid is

$$\nabla^2 \varphi_1 + k_{p1}^2 \varphi_1 = 0 \quad (2)$$

for the casing and the cement sheath, the wave equations are

$$\begin{aligned} \nabla^2 \varphi_i + k_{pi}^2 \varphi_i = 0, \quad \nabla^2 \chi_i + k_{si}^2 \chi_i = 0, \\ \nabla^2 \eta_i + k_{si}^2 \eta_i = 0, \quad (i = 2, 3) \end{aligned} \quad (3)$$

where

$$k_{p1} = \frac{\omega}{v_{p1}}, \quad k_{pi} = \frac{\omega}{v_{pi}}, \quad k_{si} = \frac{\omega}{v_{si}}, \quad (i = 2, 3) \quad (4)$$

in which k_{pi} and k_{si} are wavenumber of longitudinal wave and shear wave respectively, ω is the angular frequency.

For anisotropic formation, the governing equations can not be decoupled by introducing the displacement potential functions, the equations of motion in term of displacements are

$$c_{ijkl} u_{k,jl} = \rho_4 u_{i,tt} \quad (5)$$

where c_{ijkl} is the elastic stiffnesses of anisotropic formation, comma “,” represents the partial differential with respect to its behind letter corresponding geometric coordinates, the summation convention on repeated subscripts is implied. The subscript “, tt ” means the second-order partial differential with respect to time t .

In following displacement and stress components, the superscript indicates layer number and the subscript denotes the corresponding components. At the cased hole wall $r = R_1$, both the normal displacements and stresses are continuous while the tangential stresses are zero, i.e.,

$$\begin{aligned} u_r^2(R_1) = u_r^1(R_1), \quad \sigma_{rr}^2(R_1) = \sigma_{rr}^1(R_1) = -p_1(R_1), \\ \sigma_{r\theta}^2(R_1) = 0, \quad \sigma_{rz}^2(R_1) = 0 \end{aligned} \quad (6)$$

where $p_1(R_1)$ is the acoustic pressure of the direct wave and the reflected wave in fluid at the cased hole wall.

In this paper, we assume that the cased hole is well-bonded. In this case, the interface between the casing and the cement sheath as well as the interface between the cement sheath and the formation can be considered as a fixed connection surface. The displacements and the stresses components are continuous at the interface $r = R_i$ ($i = 2, 3$)

$$\begin{aligned} \sigma_{rr}^n(R_n) = \sigma_{rr}^{n+1}(R_n), \quad \sigma_{r\theta}^n(R_n) = \sigma_{r\theta}^{n+1}(R_n), \\ \sigma_{rz}^n(R_n) = \sigma_{rz}^{n+1}(R_n), \quad u_r^n(R_n) = u_r^{n+1}(R_n), \\ u_\theta^n(R_n) = u_\theta^{n+1}(R_n), \quad u_z^n(R_n) = u_z^{n+1}(R_n), \end{aligned} \quad (7)$$

$$(n = 2, 3)$$

Therefore, the whole problem can be generalized as to solve the governing equations (2), (3) and (5) under the boundary condition (6) and (7). Owing to the difficulty to solve the equations of motion in general anisotropic formation analytically,

the approximation method is applied here. Actually, what we concern in sonic logging is borehole modes such as Stoneley wave and flexural wave. The perturbation integral procedure can be employed to calculate the changes in eigenfrequency of modes caused by the anisotropy of the formation. This method is first proposed by Sinha and Norris [Sinha and Norris (1994)] to aim at the open hole case, it is also suitable for the cased hole [Li, Wang, Liu, Cao, Lu, Xie, Liu, and Lu (2006)].

Here we present a simple derivation of a perturbation model specifically adapted for the waves propagating along a cased hole. Before considering the specific problem of the cased hole, some general results are presented for an arbitrary volume V of anisotropic elastic material bounded by the surface S . The steady-state form of the motion equations in anisotropic medium of interest is

$$c_{ijkl}u_{k,jl} + \rho\omega^2 u_i = 0 \quad (8)$$

where c_{ijkl} is the elastic stiffnesses and ρ is the mass density of the anisotropic medium in perturbed state. Assuming the corresponding equations in unperturbed reference model is

$$c_{ijkl}^0 u_{k,jl}^0 + \rho^0 (\omega^0)^2 u_i^0 = 0 \quad (9)$$

where c_{ijkl}^0 is the elastic stiffnesses of unperturbed or reference model with density ρ^0 , u_i^0 denotes a harmonic solution at frequency ω^0 . The subscript "0" refers all quantities to the unperturbed reference state. The parameters and solutions of the anisotropic model of interest in perturbed state may be expressed as those of the reference model in unperturbed state plus a small perturbation

$$\begin{aligned} c_{ijkl} &= c_{ijkl}^0 + \varepsilon c'_{ijkl}, & \rho &= \rho^0 + \varepsilon \rho', \\ u_i &= u_i^0 + \varepsilon u'_i, & \omega &= \omega^0 + \varepsilon \omega' \end{aligned} \quad (10)$$

where ε is a small perturbation parameter, defined by the relative difference between the perturbed elastic stiffnesses c_{ijkl} and unperturbed elastic stiffnesses c_{ijkl}^0 . Differing from weak material anisotropy as defined by Thomsen [Thomsen (1986)], the small perturbation parameter in this context depends on the choice of the unperturbed elastic constants and it can be made progressively smaller by selecting the unperturbed

elastic constants closer to the perturbed constants [Sinha and Norris (1994)].

Taking the inner product in both sides of equation (8) with u_i^* , integrating over the volume V , using the perturbational expressions in equations (10), applying the traction free boundary conditions that borehole waves decay away from the borehole in both unperturbed and perturbed state [Sinha and Kostek (1996)], and keeping terms up to the first-order approximation about ε , we obtain

$$\omega' = \frac{\int_V c'_{ijkl} u_{k,l}^0 (u_{i,j}^0)^* dV}{2\omega^0 \int_V \rho^0 u_i^0 (u_i^0)^* dV} - \frac{\omega^0 \int_V \rho' u_i^0 (u_i^0)^* dV}{2 \int_V \rho^0 u_i^0 (u_i^0)^* dV} \quad (11)$$

where $*$ denotes complex conjugate. For a cased hole, the volume integral in equation (11) should be carried out layer by layer. If let $\rho = \rho^0$, then $\rho' = 0$, the second term of the right-hand side in equation (11) vanishes. The alteration in phase velocity caused by anisotropic formation can be gained according to the relation $v = \omega/k$. Considering the displacement can be written as variable separable form $u^0(r, \theta, z) = \hat{u}^0(r, \theta) e^{ikz}$, the z integral may be eliminated in equation (11). At last, the equation (11) can be expressed explicitly in the cylindrical coordinates as

$$\begin{aligned} \frac{v'}{v^0} &= \frac{v - v^0}{v^0} = \frac{\omega'}{\omega^0} \\ &= \frac{\int_{R_3}^{\infty} r dr \int_0^{2\pi} d\theta [c'_{ijkl} \hat{u}_{k,l}^0 (\hat{u}_{i,j}^0)^*]}{2(\omega^0)^2 \sum_{n=1}^4 \int_{R_{n-1}}^{R_n} r dr \int_0^{2\pi} d\theta [\rho^0 \hat{u}_i^0 (\hat{u}_i^0)^*]} \end{aligned} \quad (12)$$

where $R_0 = 0$ is the inside radius of the fluid in cased hole, $R_4 = \infty$ is the outer radius of the formation, v^0 and v are phase velocity of zero-order cased hole mode in unperturbed and perturbed state respectively. Because only the anisotropic formation contributes to the alterations in phase velocity of cased borehole waves, the integral is carried out merely in the formation for the numerator of equation (12).

Before applying equation (12), the elastic constants of the ideal model in unperturbed or reference state should be determined. Considering both the casing and the cement sheath are

isotropic, their elastic constants in unperturbed state are completely identical with those in perturbed state. The equivalent isotropic elastic constants μ and λ of reference formation in unperturbed state can be obtained from the plane wave velocities along cased hole axis in anisotropic formation. For the qSH and qSV polarized flexural waves propagating along the cased hole axis, the equivalent isotropic elastic constants of reference formation in unperturbed state are given respectively as [Sinha and Norris (1994)]

$$\begin{aligned} \mu_{\text{qSH}} &= \rho_4 V_{\text{qSH}}^2, & \lambda_{\text{qSH}} &= \rho_4 (V_{\text{qP}}^2 - 2V_{\text{qSH}}^2) \\ \mu_{\text{qSV}} &= \rho_4 V_{\text{qSV}}^2, & \lambda_{\text{qSV}} &= \rho_4 (V_{\text{qP}}^2 - 2V_{\text{qSV}}^2) \end{aligned} \quad (13)$$

where V_{qP} , V_{qSV} and V_{qSH} are plane wave velocities along the cased hole axis in anisotropic formation. The subscript qSH and qSV denote the equivalent isotropic elastic constants for the qSH and qSV polarized flexural wave in cased hole, respectively. These equivalent isotropic parameters serve to define the flexural wave solutions in the reference or unperturbed state. Any contribution to the dispersion of cased hole flexural waves because of the differences in the elastic constants of the anisotropic and the equivalent isotropic formation is accounted for in the perturbation model discussed earlier. This choice of equivalent isotropic elastic constants may make the perturbative correction minimal, which results in high accuracy of perturbed solution [Sinha and Norris (1994)].

In this paper, the Thomsen-Haskell transfer matrix method is adopted to calculate the dispersion relations of flexural waves in cased hole in unperturbed or reference isotropic formation firstly before using equation (12).

3 Numerical computation and results

At last, we provide a numerical example. A schematic of a cased hole and the global coordinate system xyz are shown in Figure 2. The casing and the cement sheath are isotropic and the TI symmetry axis of the formation is in xz plane and makes an angle φ with the cased hole axis z . Establishing the local Cartesian coordinate $x'y'z'$ in

formation, z' axis coincides with the TI symmetry axis and y' axis is parallel to y axis in global coordinate system.

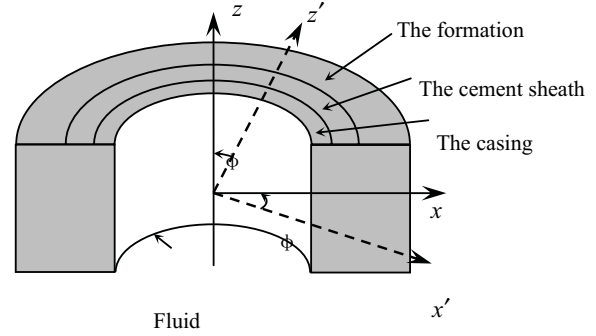


Figure 2: A fluid-filled cased hole in TI formation

The elastic modulus matrix of formation in local Cartesian coordinate system is

$$C_{\text{local}} = \begin{pmatrix} C_{11} & C_{12} & C_{13} & 0 & 0 & 0 \\ C_{12} & C_{11} & C_{13} & 0 & 0 & 0 \\ C_{13} & C_{13} & C_{33} & 0 & 0 & 0 \\ 0 & 0 & 0 & C_{44} & 0 & 0 \\ 0 & 0 & 0 & 0 & C_{44} & 0 \\ 0 & 0 & 0 & 0 & 0 & \frac{C_{11}-C_{12}}{2} \end{pmatrix} \quad (14)$$

where C_{11} , C_{12} , C_{13} , C_{33} and C_{44} are five independent elastic stiffnesses for TI formation. The elastic modulus matrix in global Cartesian coordinate can be obtained by coordinate transformation through introducing a 6×6 transformation matrix M [Auld, (1973)]

$$M = \begin{pmatrix} \cos^2 \varphi & 0 & \sin^2 \varphi & 0 & \sin 2\varphi & 0 \\ 0 & 1 & 0 & 0 & 0 & 0 \\ \sin^2 \varphi & 0 & \cos^2 \varphi & 0 & -\sin 2\varphi & 0 \\ 0 & 0 & 0 & \cos \varphi & 0 & -\sin \varphi \\ -\frac{1}{2} \sin 2\varphi & 0 & \frac{1}{2} \sin 2\varphi & 0 & \cos 2\varphi & 0 \\ 0 & 0 & 0 & \sin \varphi & 0 & \cos \varphi \end{pmatrix} \quad (15)$$

then, the elastic modulus matrix of formation in global Cartesian coordinate system is

$$C_{\text{global}} = M C_{\text{local}} M^T \quad (16)$$

where M^T is the transpose of matrix M .

The cylindrical coordinate is always adopted for the borehole problem. Therefore, the elastic modulus matrix of formation in global Cartesian coordinate should be transformed into cylindrical coordinate, the transformation matrix $M_{\text{cylindrical}}$ is

$$M_{\text{cylindrical}} = \begin{pmatrix} \cos^2 \theta & \sin^2 \theta & 0 & 0 & 0 & \sin 2\theta \\ \sin^2 \theta & \cos^2 \theta & 0 & 0 & 0 & -\sin 2\theta \\ 0 & 0 & 1 & 0 & 0 & 0 \\ 0 & 0 & 0 & \cos \theta & -\sin \theta & 0 \\ 0 & 0 & 0 & \sin \theta & \cos \theta & 0 \\ -\frac{1}{2} \sin 2\theta & \frac{1}{2} \sin 2\theta & 0 & 0 & 0 & \cos 2\theta \end{pmatrix} \quad (17)$$

the elastic modulus matrix of formation in cylindrical coordinate can be expressed as

$$C_{\text{cylindrical}} = M_{\text{cylindrical}} C_{\text{global}} M_{\text{cylindrical}}^T \quad (18)$$

According to equation (18), the elastic matrix of formation in cylindrical coordinate has a complex relation with angle θ if the TI symmetry axis is not parallel to the cased hole axis, which can be said in a simpler way that with a tilted axis of symmetry, the formation is azimuthally anisotropic. That is the main reason that the equations of motion in anisotropic media cannot be solved analytically.

The material and geometric parameters of cased hole and TI formation are listed in Table 1 and Table 2.

The procedure to compute the dispersion curves of cased hole flexural waves in anisotropic formation is: (1) calculate the plane-wave velocities in anisotropic formation and obtain the equivalent elastic constants of reference isotropic formation from the equation (13); (2) compute the dispersion relation of cased hole flexural waves in unperturbed or reference isotropic formation using transfer matrix method, and the displacement solutions in unperturbed state is also obtained simultaneously; (3) calculate the changes in phase velocity of cased hole flexural waves in anisotropic formation according to equation (12), then the dispersion curves can be obtained.

According to the computational parameters in Table 1 and Table 2, Figures 3 and 4, respectively, show qP, qSV and SH wave velocities in fast and slow TI formation as a function of propagation direction from the TI symmetry axis.

Figures 5 and 6 illustrate the dispersion curves of qSV and SH polarized case hole flexural waves in fast and slow TI formation respectively for four different inclinations of the cased hole with respect to the TI symmetry axis of formation. The corresponding dispersion curves of open hole flexural waves are displayed in Figures 7 and Figure 8 for comparison. Here the dispersion curves in Figure 7 are perfectly agreement with the corresponding curves obtained by Sinha and Norris [Sinha and Norris (1994)], which indicates the computational results in this paper are correct.

Comparing Figure 5 with 7, and Figure 6 with 8, the form of dispersion curves for cased hole and open hole are similar in fast TI formation while much different in slow TI formation. In addition, the cut-off frequency for flexural waves in cased hole is always higher than that for open hole, especially in slow TI formation. That means the influence of the casing and the cement sheath on dispersion curves of flexural wave is much greater in slow TI formation than in fast TI formation.

In the open hole situation, from Figure 7, both qSV and SH polarized flexural wave dispersion curves for the different borehole inclinations in fast TI formation coalesce gradually with the frequency increase and tend toward a definite value at higher frequencies. While from Figure 8, both qSV and SH polarized flexural waves in slow TI formation exhibit a rather uniform spread at higher as well as lower frequencies. Unlike the open hole, in the cased hole case, from Figures 5 and 6, the velocity of all the qSV and SH polarized flexural waves in both fast and slow TI formation approach a definite value uniformly at higher frequencies. At the same frequency arbitrary, the velocity of flexural waves in cased hole is always greater than the corresponding flexural wave velocity in open hole.

The above results indicate that the high-frequency flexural wave velocity in both open hole and cased

Table 1: The cased hole model parameters

Parameter	$v_p/(m/s)$	$v_s/(m/s)$	ρ (Kg/m ³)	$R_{n-1}/(m)$	$R_n/(m)$
The fluid	1500		1000	0	0.0635
The casing	6098	3354	7500	0.0635	0.0715
The cement	2823	1729	1920	0.0715	0.1016

Table 2: The TI stratum parameters

Parameter	$C_{11}/(GPa)$	$C_{12}/(GPa)$	$C_{13}/(GPa)$	$C_{33}/(GPa)$	$C_{44}/(GPa)$	ρ (Kg/m ³)
Fast stratum	40.9	10.3	8.5	26.9	10.5	2230
Slow stratum	20.58	10.68	5.04	11.2	4.75	2200

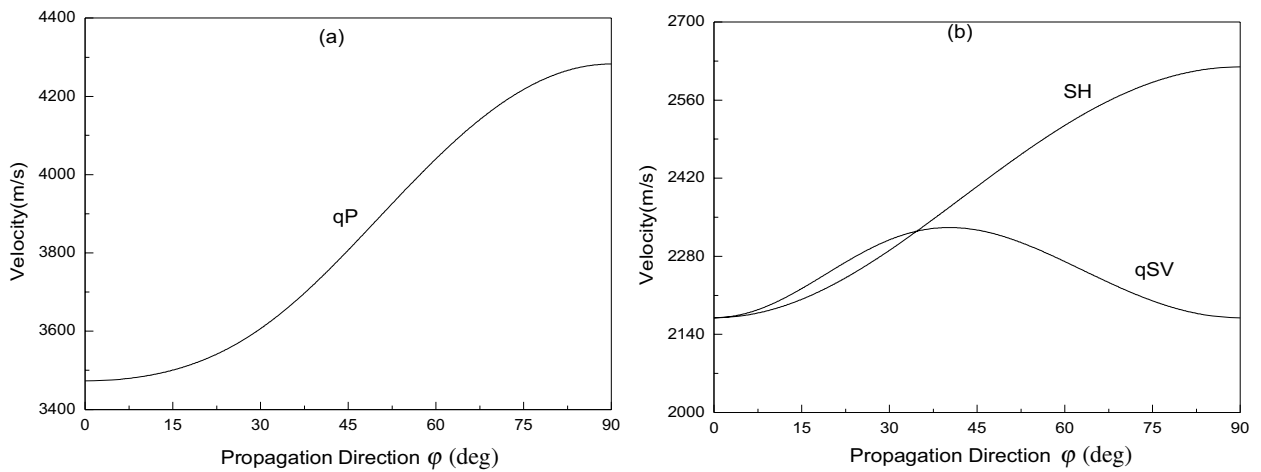


Figure 3: The plane wave velocity in fast TI formation as a function of propagation direction from the TI symmetry axis. (a) qP wave velocity, (b) qSV and SH wave velocity

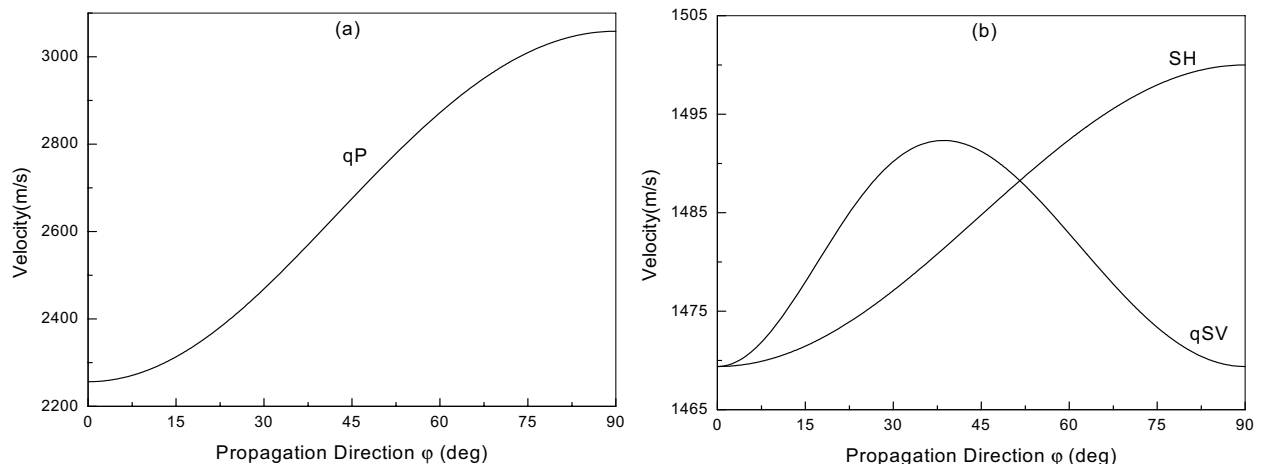


Figure 4: The plane wave velocity in slow TI formation as a function of propagation direction from the TI symmetry axis. (a) qP wave velocity, (b) qSV and SH wave velocity

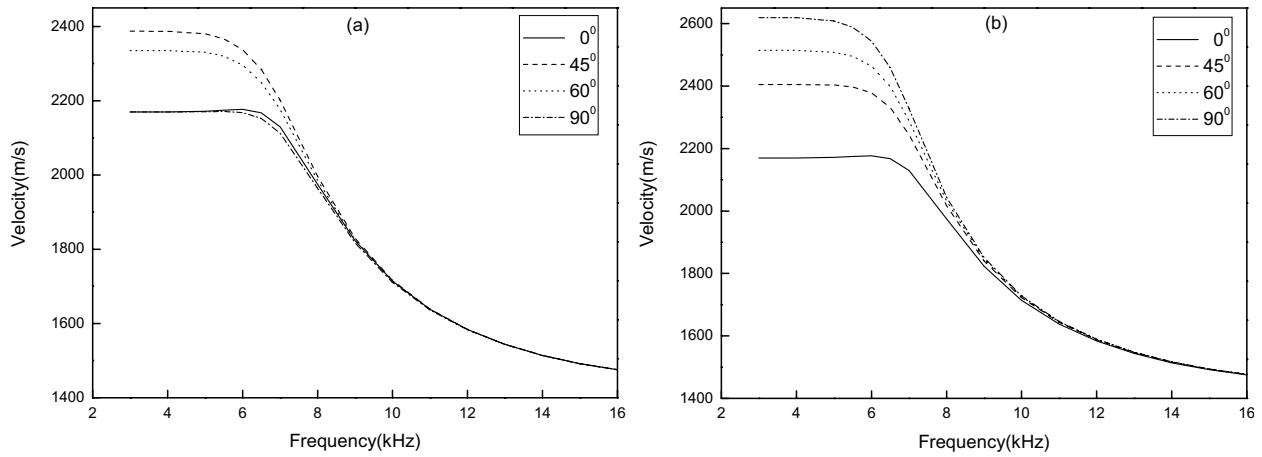


Figure 5: Dispersion curves for cased hole flexural waves in fast TI formation with different inclinations (a) qSV polarized cased hole flexural wave, (b) SH polarized cased hole flexural wave

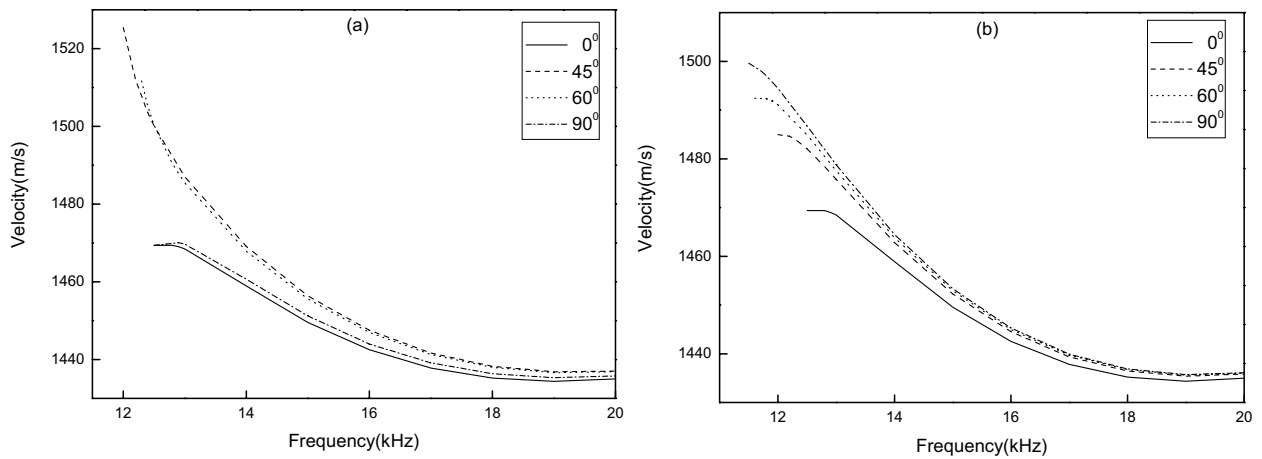


Figure 6: Dispersion curves for cased hole flexural waves in slow TI formation with different inclinations (a) qSV polarized cased hole flexural wave, (b) SH polarized cased hole flexural wave

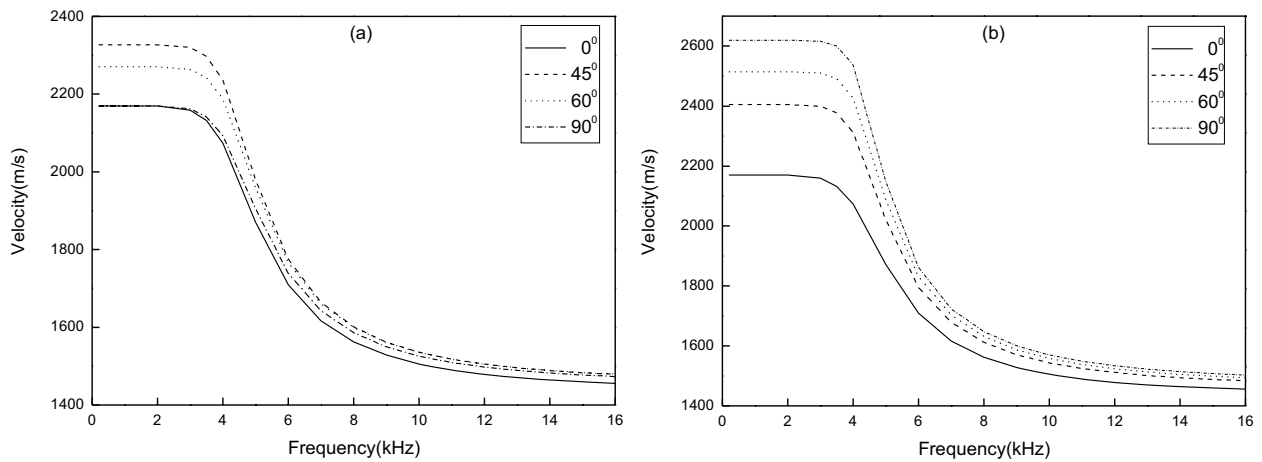


Figure 7: Dispersion curves for open hole flexural waves in fast TI formation with different inclinations (a) qSV polarized open hole flexural wave, (b) SH polarized open hole flexural wave

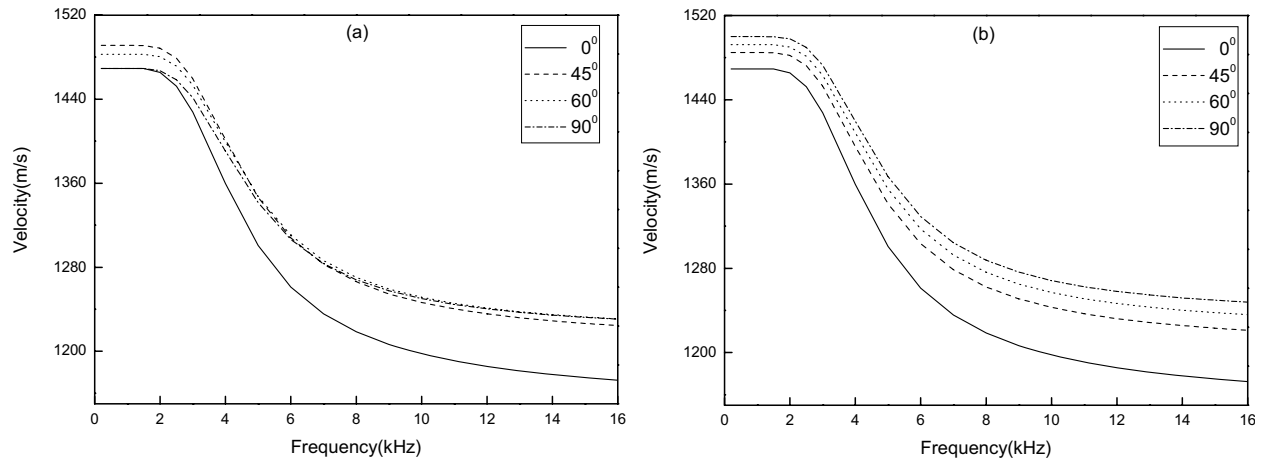


Figure 8: Dispersion curves for open hole flexural waves in slow TI formation with different inclinations (a) qSV polarized open hole flexural wave, (b) SH polarized open hole flexural wave

hole are all close to their corresponding Stoneley wave speed. Because the Stoneley wave is a interface wave, in the open hole condition, the interface is the one between the borehole liquid and anisotropic formation. Since the Stoneley wave velocity in open hole in fast formation essentially approach to the compressional speed in the liquid when the frequency is high enough, all these flexural wave dispersion curves will close together gradually with the frequency increase. Whereas the Stoneley wave velocity in open hole in slow formation relates to the anisotropic constants of the surrounding formation, the high-frequency asymptotes of the flexural wave dispersion curves for the different borehole inclination are also dissimilar.

In the cased hole situation, the interface for Stoneley wave is the one between the borehole liquid and the casing. The casing is the fast medium, so the Stoneley wave velocities at higher frequencies in slow TI formation are almost equal to those in fast TI formation, which are compressional speed in the liquid and independent of the inclination of the borehole respect to the TI symmetry axis. Therefore, the high-frequency asymptotes of the flexural wave velocities of cased hole are also nearly identical both in fast and slow TI formation. For the Stoneley wave in cased hole, integrate the properties of the casing whatever the frequency and is thus faster than in the open hole. Thus, the flexural wave velocity in cased hole is

always higher than the corresponding velocity in open hole at same frequency.

In both the open hole and cased hole, at a frequency high enough, the phase velocity of both Stoneley and the flexural modes tend toward that of the appropriate Scholte wave.

4 Conclusion

Based on the perturbation method and the Thomson-Haskell transfer matrix method, the flexural wave dispersion curves of well-boned cased hole in anisotropic formation are investigated. The numerical results show that comparing to the open hole situation, the existence of the casing and the cement sheath makes the cut-off frequency of flexural waves in cased hole move to higher frequency, especially in slow formation. Integrating the properties of the casing, the flexural wave in cased hole is always faster than in the open hole at arbitrarily same frequency. Unlike the open hole situation, the high-frequency asymptotes of the flexural wave dispersion curves in both fast and slow TI formation with different inclinations are all almost close to an identical fluid-casing interface Stoneley wave velocity. The flexural wave and Stoneley wave in both open hole and cased hole reach the appropriate Scholte wave velocity at a frequency high enough.

Acknowledgement: Project supported by the

Special Science Foundation of the Doctoral Discipline of the Ministry of Education of China (No.20050001016)

References

- Alturi, S. N.; Liu, H. T.; Han, Z. D.** (2006): Meshless local Petrov-Galerkin (MLPG) mixed finite difference method for solid mechanics, *CMES: Computer Modeling in Engineering and Sciences*, **15**(1), 1-16.
- Auld, B. A.** (1973): *Acoustic fields and Waves in Solids*, vol. 1, John Wiley and Sons, Inc.
- Ellefsen, K. J.; Cheng, C. H.; Toksoz, M. N.** (1991): Applications of perturbation theory to acoustic logging, *J. Geophys. Res.*, **96**(B1), 537-549.
- Ellefsen, K. J.; Cheng, C. H.; Toksoz, M. N.** (1991): Effects of anisotropy upon the normal modes in a borehole, *J. Acoust. Soc. Am.*, **89**, 2597-2616.
- Gao, L.; Liu, K.; Liu, Y.** (2006): Application of MLPG method in dynamic fracture problems, *CMES: Computer Modeling in Engineering and Sciences*, **12**(3), 181-195.
- Leslie, H. D.; Randall, C. J.** (1992): Multipole sources in boreholes penetrating anisotropic formations: Numerical and experimental results, *J. Acoust. Soc. Am.*, **91**, 12-27.
- Li, G.; Wang, K. X.; Liu, J. X.; Cao, Z. L.; Lu, G. W.; Xie, R. H.; Liu, J. S.; Lu, X. M.** (2006): Acoustoelasticity theory, numerical analysis and practical example of the cased hole with stress concentration by cross-dipole acoustic logging, *Chinese J. Geophysics*, **49**(1), 295-304.
- Liu, Q. H.; Sinha, B. K.** (2003): A 3D cylindrical PML/FDTD method for elastic waves in fluid-filled pressurized boreholes in triaxially stressed formations, *Geophysics*, **68**(5), 1731-1743.
- Norris, A. N.; Sinha, B. K.** (1996): Anisotropy-induced coupling in borehole acoustic modes, *J. Geophys. Res.*, **101**(B7), 15945-15952.
- Schmitt, D. P.** (1988): Shear wave logging in elastic formations, *J. Acoust. Soc. Am.*, **84**, 2215-2229.
- Schmitt, D. P.** (1993): Dipole logging in cased boreholes, *J. Acoust. Soc. Am.*, **93**, 640-657.
- Sinha, B. K.; Norris, A. N.; Chang, S. H.** (1994): Borehole flexural modes in anisotropic formations, *Geophysics*, **59**(7), 1037-1052.
- Sinha, B. K.; Kostek, S.** (1996): Stress-induced azimuthal anisotropy in borehole flexural waves, *Geophysics*, **61**(6), 1899-1907.
- Sladek, J.; Sladek, V.; Atluri, S. N.** (2004): Meshless local Petrov-Galerkin method in anisotropic elasticity, *CMES: Computer Modeling in Engineering and Sciences*, **6**(5), 477-489.
- Thomsen, L.** (1986): Weak elastic anisotropy, *Geophysics*, **51**, 1954-1966.
- Tubman, K. M.; Cheng, C. H.; Toksoz, M. N.** (1984): Synthetic full waveform acoustic logs in cased boreholes, *Geophysics*, **49**, 1051-1059.
- Tubman, K. M.; Cheng, C. H.; Cole, S. P.; Toksoz, M. N.** (1986): Synthetic full waveform acoustic logs in cased boreholes- II. Poorly bonded casing, *Geophysics*, **51**, 902-913.
- Zhang, B. X.; Wang, K. X.** (1996): Theoretical study of perturbation method for acoustic multipole logging in anisotropic formation, *J. Acoust. Soc. Am.*, **99**(5), 2674-2685.
- Zhang, B. X.; Wang, K. X.** (2000): Theoretical study of multipole acoustic logging in anisotropic two-phase medium formation, *Chinese Journal of Geophysics*, **43**(5), 707-718.